European Journal of Neuroscience, Vol. 7, pp. 1188–1198, 1995

Glycine- and GABA-activated Currents in Identified Glial Cells of the Developing Rat Spinal Cord Slice

Andrea Pastor[1], Alexandr Chvátal[2], Eva Syková[2] and Helmut Kettenmann[3]
[1]Institute of Neurobiology, University of Heidelberg, Im Neuenheimer Feld 345, 69120 Heidelberg, Germany
[2]Laboratory of Cellular Neurophysiology, Institute of Experimental Medicine, Academy of Sciences of the Czech Republic, Videnska 1083, CS-142 20, Prague 4, Czech Republic
[3]Max Delbrück Centre for Molecular Medicine, Robert-Rössle-Strasse 10, 13122 Berlin, Germany

Keywords: astrocytes, oligodendrocytes, patch clamp, development, precursor cells

Abstract

In the neonatal rat spinal cord, four types of glial cells, namely astrocytes, oligodendrocytes and two types of precursor cells, can be distinguished based on their membrane current patterns and distinct morphological features. In the present study, we demonstrate that these cells respond to the inhibitory neurotransmitters glycine and GABA, as revealed with the whole-cell recording configuration of the patch-clamp technique. All astrocytes and glial precursor cells and a subpopulation of oligodendrocytes responded to glycine. The involvement of glycine receptors was inferred from the observation that the response was blocked by strychnine and that the induced current reversed close to the Cl^- equilibrium potential. GABA induced large membrane currents in astrocytes and precursor cells while oligodendrocytes showed only small responses. The GABA-activated current was due to the activation of $GABA_A$ receptors since muscimol mimicked and bicuculline blocked the response; moreover, the reversal potential was close to the Cl^- equilibrium potential. Besides the increase in a Cl^- conductance, $GABA_A$ receptor activation also induced a block of the resting K^+ conductance, as observed previously in Bergmann glial cells. Our experiments show that while glial $GABA_A$ receptors are found in many brain regions and the spinal cord, glial glycine receptors have so far been detected only in the spinal cord. The restricted coexpression of glial and neuronal glycine receptors in a defined central nervous system grey matter area implies that such glial receptors may be involved in synaptic transmission.

Introduction

Spinal cord glial cells express a variety of voltage-gated channels and receptors in culture (e.g. Kettenmann *et al.*, 1983; Sontheimer and Kettenmann, 1988; Sontheimer and Waxman, 1992; Thio *et al.*, 1993) and in a brain slice preparation (Chvátal *et al.*, 1995). Among these are voltage-gated K^+ and Na^+ channels (Sontheimer *et al.*, 1992; Chvátal *et al.*, 1995) and receptors for GABA and glutamate (Gilbert *et al.*, 1984). These findings are in line with the developing concept that glial cells from the central nervous system are diverse with respect to their electrophysiological behaviour and that they are equipped with a large repertoire of voltage-gated channels and transmitter receptors. The receptors are thought to be involved in non-synaptic events such as the control of proliferation (Condorelli *et al.*, 1989), the extent of the glial communication via gap junctions (Giaume *et al.*, 1991) and the control of extracellular ion homeostasis (Bormann and Kettenmann, 1988). Recent evidence, however, suggests that impairment of glial cell function has a profound effect on synaptic transmission (Keyser and Pellmar, 1994). This study implied that glial cells exert strong control on the strength of synaptic function. To develop specific concepts on a glial contribution in synaptic transmission, the expression pattern of glial transmitter receptors and their distribution in the normal and developing brain needs to be studied. The majority of previous studies were performed in cell cultures. Since cultured cells are not surrounded by their normal environment, neuron–glia interactions cannot be properly analysed in culture. Studies in brain slices can better mirror the complex situation *in vivo*.

In a previous study, we used a brain slice preparation of the spinal cord to access spinal cord glial cells *in situ*. Four cell types were distinguished and characterized as astrocytes, oligodendrocytes, and precursor cells of the astrocytic and oligodendrocytic lineages by combining the patch-clamp technique with immunocytochemical and morphological identification (Chvátal *et al.*, 1995). The four cell types expressed distinct electrophysiological properties; the patch-clamp technique can therefore be used as a tool to identify glial cell types. During postnatal development the population of mature cells—astrocytes and oligodendrocytes—increased relative to the number of glioblasts. The change in the cell population from precursors to mature glia coincides with the increasing ability of glial cells to control the K^+ and pH homeostasis in the extracellular space (Jendelova and Sykova, 1991; Sykova *et al.*, 1992) and with the decrease in extracellular space volume (Sykova and Chvátal, 1993). In spinal cord slices from postnatal days (P) 3–8 the majority of cells

Correspondence to: Helmut Kettenmann, as above

Received 11 October 1994, revised 17 December 1994, accepted 23 December 1994

showed morphological features and the electrophysiological pattern of glioblasts, while after P10 most cells expressed membrane properties of astrocytes and oligodendrocytes in concert with the distinct morphological properties of these cell types (Chvátal *et al.*, 1995). The presence of GABA receptors in Bergmann glia or corpus callosum oligodendrocytes also undergoes changes in development, as characterized in brain slices (Berger *et al.*, 1991; Müller *et al.*, 1994). So far, the expression of transmitter receptors and its developmental changes have not been studied in a slice preparation of the spinal cord. We therefore analysed the properties and developmental regulation of the two main inhibitory transmitters of the spinal cord, GABA and glycine. We demonstrate that astrocytes, oligodendrocytes and glioblasts show distinct and complex responses involving the activation of $GABA_A$ and glycine receptors.

Materials and methods

Preparation of spinal cord slices and electrophysiological setup

Young rats were killed at P3–P18 by decapitation. The spinal cords were quickly dissected out and washed in bathing solution at 8–10°C. A 3–4 mm long segment of the spinal cord was embedded in 1.7% agar (Difco, Detroit, MI). The spinal cord was cut transversely into 120–150 μm thick slices using a vibratome (FTB, Plano, Marburg, Germany). Slices were transferred to a nylon net in cold (5°C) bathing solution and were then slowly warmed up to room temperature. For electrophysiological recordings slices were placed in a chamber mounted on the stage of a Zeiss microscope (modified Standard 16; Zeiss, Oberkochen, Germany) and fixed in a chamber using a U-shaped platinum wire with a grid of nylon threads (Edwards *et al.*, 1989). The chamber was continuously perfused with oxygenated bathing solution and substances were added by changing the perfusate. Cell somata in the spinal cord slice were visible in normal water immersion optics, and could be approached by the patch electrode. The image was illuminated with infrared light and detected with an infrared-sensitive video camera (C3077; Hamamatsu Photonics, Hamamatsu City, Japan) and displayed on a standard black-and-white monitor (Dodt *et al.*, 1989).

The selected cells had a clear, dark membrane surface and were located 10–30 μm beyond the surface of the slice. Positive pressure was applied to the recording pipette while being lowered to the slice under microscopic control. The cellular debris was blown aside and the tip could be placed onto the surface of a cell soma. Membrane currents were measured with the patch-clamp technique in the whole-cell recording configuration (Hamill *et al.*, 1981). Current signals were amplified with conventional electronics (EPC-7 amplifier; List Electronics, Darmstadt, Germany), filtered at 3 kHz and sampled at 5 kHz with an interface (TIDA; Battelle Europe, Frankfurt, Germany) connected to an AT-compatible computer system which also served as a stimulus generator.

Solutions and electrodes

A standard bathing solution was used in our experiments with the following composition (in mM): NaCl 134.0, KCl 2.5, $CaCl_2$ 2.0, $MgCl_2$ 1.3, K_2HPO_4 1.25, $NaHCO_3$ 26.0, D-glucose 10.0, pH 7.4 (the total K^+ concentration was thus 5 mM). The solution was gassed with a mixture of 95% O_2 and 5% CO_2. The following transmitters and drugs were added to the standard bath solution in the concentrations as indicated in the text: 4-aminopyridine (4-AP), GABA, glycine, strychnine, (–)bicuculline methochloride, muscimol, methyl-6,7-dimethoxy-4-ethyl-β-carboline-3-carboxylate (DMCM) (Sigma, Taufkirchen, Germany) and picrotoxin (RBI, MA 01760, USA). In solution picrotoxin gives rise to the pharmacologically active component picrotoxinin and the inactive picrotin. Bicuculline, strychnine, DMCM and picrotoxin were solubilized in 100 μl dimethyl sulphoxide before adding to the bath solution.

The internal pipette solution had the following composition (in mM): KCl 130.0, $CaCl_2$ 0.5, $MgCl_2$ 2.0, EGTA 5.0, HEPES 10.0, pH 7.2. All experiments were carried out at room temperature (~22°C). Recording pipettes were fabricated from borosilicate capillaries (Hilgenberg, Malsfeld, Germany) and coated with Sigmacote (Sigma). The open resistance of these patch pipettes was 5–6 MΩ. The pipette always contained 1 mg/ml Lucifer yellow (Fluka, Buchs, Switzerland).

Intracellular staining of cells

During recording cells were filled with Lucifer yellow by dialysing the cytoplasm with the patch pipette solution. To avoid destruction of the cell by pulling off the pipette after recording, we destroyed the seal by injection of a large hyperpolarizing current pulse. After recording from the cell, the slice was fixed for 3–5 h at room temperature in 4% paraformaldehyde in 0.1 M phosphate buffer, pH 7.4. Slices were then transferred to phosphate buffer. Lucifer yellow-filled cells were examined in a fluorescence microscope equipped with a fluorescein isothiocyanate filter combination (band-pass 450–490 nm, mirror 510 nm, long pass 520 nm).

Immunocytochemistry

Indirect immunofluorescence staining was performed on spinal cord slices after electrophysiological recording and injection of Lucifer yellow. Monoclonal antibodies O1 and O4 characterized by Sommer and Schachner (1981), and antibodies to glial fibrillary acidic protein (GFAP) [Eng *et al.*, 1971; Debus *et al.*, 1983; polyclonal rabbit-anti-human GFAP (Prof. L. F. Eng, Department of Pathology, Stanford University of Medicine, Palo Alto, CA) and monoclonal mouse-antihuman GFAP (Böhringer, Mannheim, Germany)] were used in this study to identify oligodendrocytes and astrocytes respectively. The binding of O1 and O4 antibodies was visualized with goat antimouse immunoglobulin antibodies coupled to Texas red and GFAP either with pig anti-rabbit immunoglobulin antibodies coupled to rhodamine or with goat antimouse immunoglobulin antibodies coupled to the chromophore Cy3.

Results

The glial cells can be identified based on their electrophysiological properties

Four types of glial cells have been distinguished in the grey matter of rat spinal cord slices at P1–P19, based on their membrane current patterns and morphological or immunohistochemical features: astrocytes, oligodendrocytes, and two types of precursor glial cells (Chvátal *et al.*, 1995). The cells were approached randomly with the patch pipette, and in the whole-cell recording configuration identified as glial in that current pulses of up to 480 pA depolarized the glial cells up to 70 mV and did not activate action potentials. In none of the cells was spontaneous electrical activity observed. In the voltage-clamp mode, currents were activated by clamping the membrane from the holding potential of −70 mV to values ranging from 20 to −160 mV. The electrophysiologically characterized cells were dialysed and thereby filled with Lucifer yellow (Fig. 1).

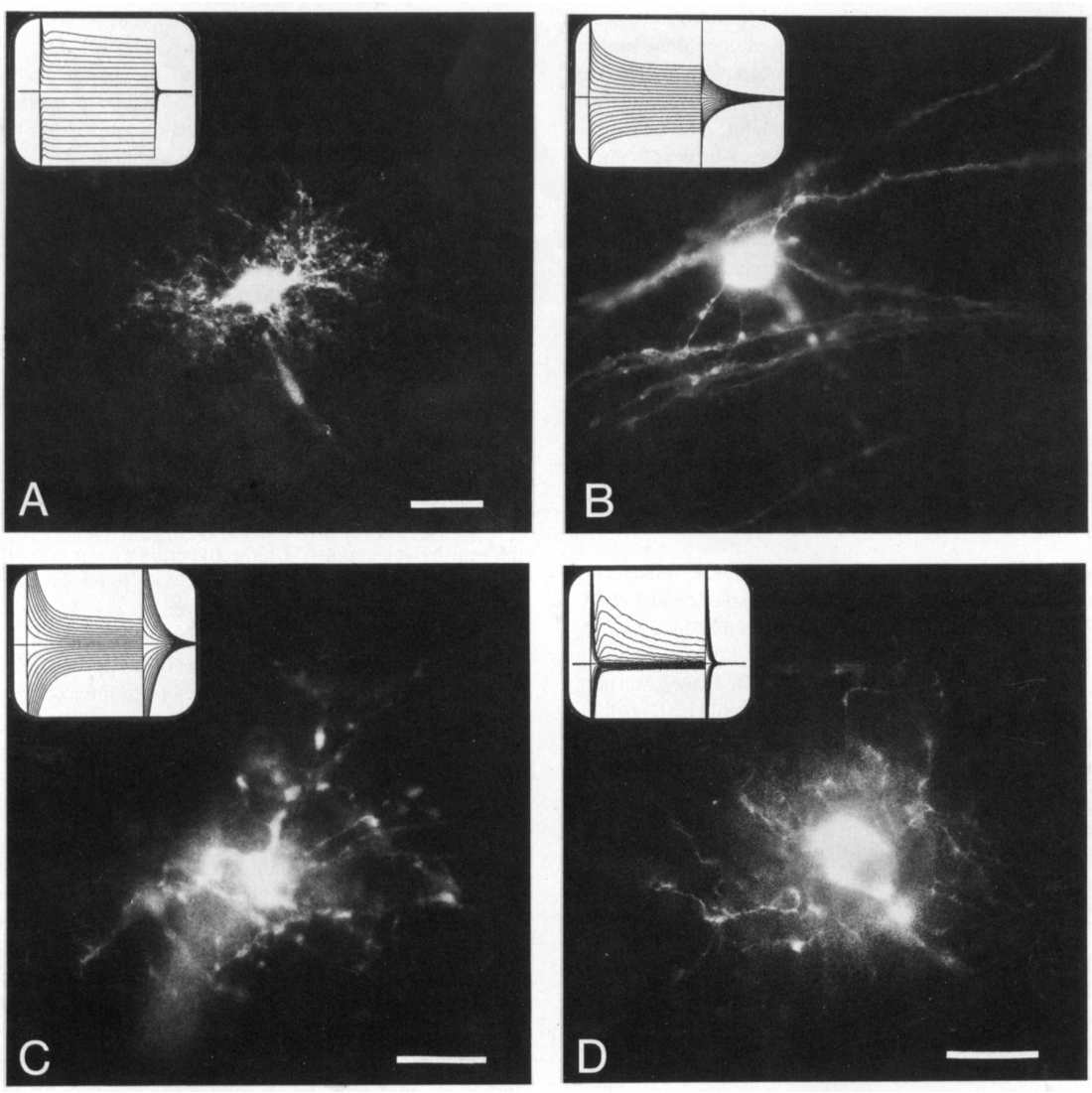

FIG. 1. Morphology and membrane current patterns of rat spinal cord glial cells. Glial cells from spinal cord slices were filled with Lucifer yellow to illustrate their morphological features. Four types were selected based on their distinct channel patterns as shown in the insets. The membrane was clamped at depolarizing potentials (–70, −60, −50, −40, −30, −20, −10, 0, 10, 20 mV) and hyperpolarizing potentials (–80, −90, −100, −110, −120, −130, −140, −150, −160 mV) for 50 ms from a holding potential of −70 mV. (A) An astrocyte from P3 is characterized by a passive current pattern on which is superimposed a slight voltage-activated component in the de- and hyperpolarizing directions. The Lucifer yellow injection reveals the arborized processes forming network-like structures. Glycine (1 mM) activated an inward current of 23 pA at a holding potential of −70 mV (not shown). The resting membrane potential (V_r) was −73 mV. (B) An oligodendrocyte from P11 identified by its passive decaying currents has long, rarely branched processes which are aligned in parallel. The glycine response was 15 pA; V_r was −70 mV. (C) An oligodendrocyte precursor cell from P9 is characterized by voltage-gated K^+ channels and no apparent response to glycine. V_r was −60 mV. (D) A glial cell with Na^+ currents from P14 responded to glycine with an inward current of 50 pA. V_r was −43 mV. Bar denotes 18 μm.

Astrocytes were characterized by symmetrical passive K^+ currents in the depolarizing and hyperpolarizing directions, on which sometimes small voltage-gated currents with properties of inwardly rectifying (K_{IR}), delayed outwardly rectifying (K_{DR}) and A-type K^+ currents (K_A) (Figs 1, 6A and 7B) were superimposed. They possessed a diffuse network of fine processes surrounding the cell soma (Fig. 1). Some cells were positively stained for GFAP (n = 6 of 20), while none showed positive labelling with a combination of O1 and O4 antibodies. Oligodendrocytes showed symmetrical passive but decaying K^+ currents, and they had long and smooth processes usually oriented in parallel (Fig. 1). These cells were positively labelled with O1/O4 antibodies (n = 9 of 18), while they were negative for the GFAP antigen (n = 8). Glial precursor cells of the oligodendrocyte lineage, which were (partially) positive for the O4 antigen (n = 3 of 11), were distinguished by the presence of K_{IR}, K_{DR} and K_A currents. The fourth type of glial cells were most likely astrocytic precursors, since some cells were labelled by GFAP (n = 3 of 14). These cells were electrophysiologically distinguishable from the oligodendrocyte precursors by the presence of Na^+ currents. The Na^+ currents were, however, at least ten times smaller than in neurons.

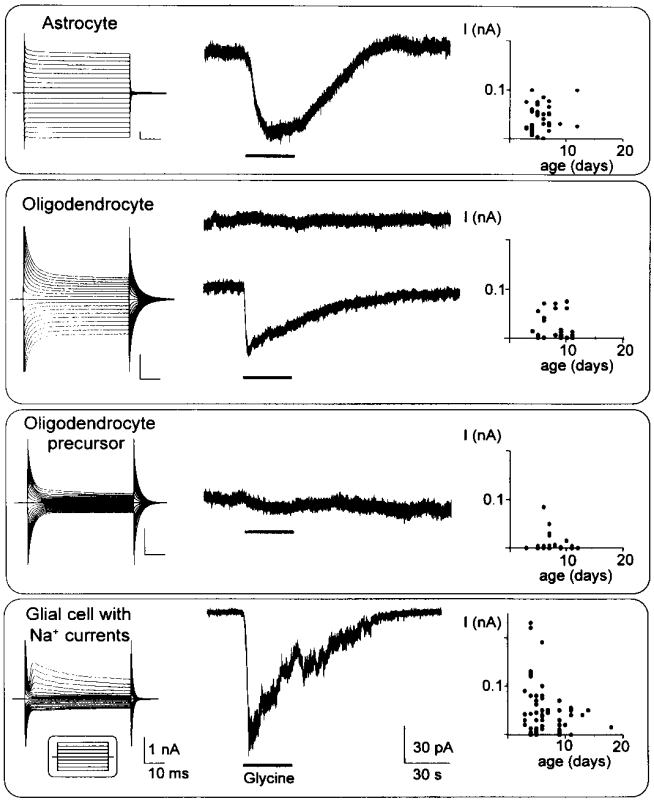

FIG. 2. Glycine responses in the four types of spinal cord glial cells during postnatal development. Cells were voltage-clamped at −70 mV and the membrane was stepped to de- and hyperpolarizing potentials as indicated in the inset at the bottom of the left row. The resulting current patterns are shown on the left. The current responses to glycine (1 mM; bar indicates application) are shown in the middle. For oligodendrocytes, glycine responses of two cells are displayed, one responsive to glycine and the other not responsive. The current patterns on the left correspond to the responsive cell. On the right, the peak amplitudes of glycine-induced inward currents are summarized from a large number of experiments and are plotted as a function of the age of the animal from which the slice was taken. Note the difference in the calibrations for the voltage-activated currents. The glycine responses are shown with the same calibration. Top panel, P7 astrocyte, resting membrane potential (V_r) −77 mV; top trace in second panel, P6 oligodendrocyte, V_r −64 mV; bottom trace in second panel, P8 oligodendrocyte, −70 mV; third panel, P12 oligodendrocyte precursor cell, V_r −64 mV; bottom panel, P6 glial cell with Na^+ current, V_r −72 mV.

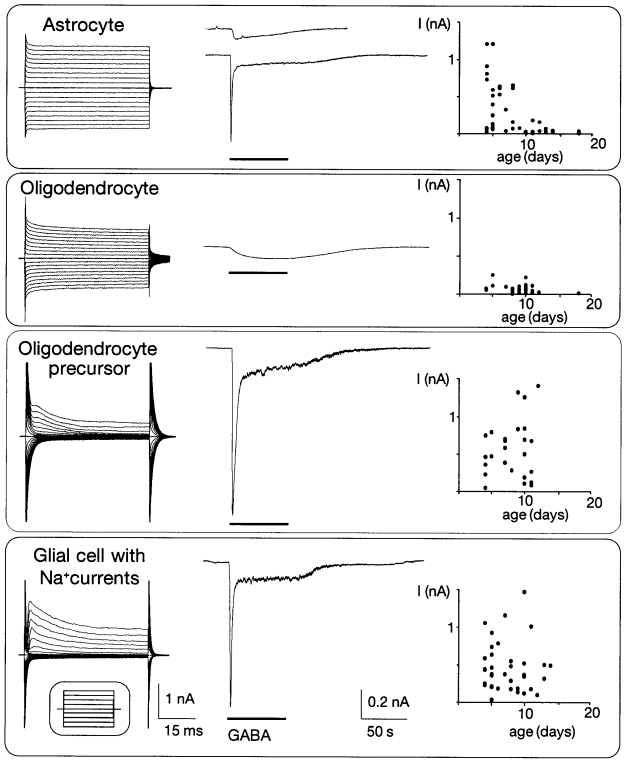

FIG. 3. GABA responses in the four types of spinal cord glial cells during postnatal development. The typical membrane current pattern (left), the response to GABA (middle, 1 mM) and the size of the GABA current as a function of the age of the animal (right) are shown for the four types of glial cells. For astrocytes, responses from two cells are displayed. The current pattern on the left corresponds to the bottom GABA response. Top trace in top panel, P10 astrocyte, resting membrane potential (V_r) −79 mV; bottom trace in top panel, P4 astrocyte, V_r −65 mV; second panel, P11 oligodendrocyte, V_r −73 mV; third panel, P11 oligodendrocyte precursor cell, V_r −65 mV; bottom panel, P7 glial cell with Na^+currents, V_r −50 mV.

Glycine and GABA activate membrane currents in astrocytes, oligodendrocytes and glial precursor cells

To study the sensitivity of the glial membrane for GABA and glycine, the transmitters were added to the perfusion medium while clamping the membrane potential at −70 mV. The majority of the glial cells responded with the activation of an inward current.

Among the astrocytes, 91% of cells (n = 33) responded to glycine application (1 mM) and 95% of cells to GABA (between 10 μM and 1 mM; n = 43). The amplitude of the glycine-activated inward currents (mean 42 ± 26 pA) did not differ among cells obtained from P3–P8 compared to P9–P18 (Fig. 2). GABA application evoked significantly larger currents than glycine, and the current amplitudes were considerably larger in cells from P3–P8, namely 400 ± 350 pA (mean ± SE, n = 27), compared to cells from more mature animals at P9–P18 (mean 41 ± 48 pA, n = 16) (Fig. 3).

Forty-eight percent of oligodendrocytes (n = 25) responded to glycine application and 94% (n = 34) to GABA. Glycine and GABA application evoked small currents, in the range of 10–75 and 10–250 pA (mean 58 ± 60 and 58 ± 49 pA) respectively. There was no apparent difference between cells from P3–P8 and those from P9–P14 (Figs 2 and 3).

Only in 20% (n = 38) of the oligodendrocyte precursor cells did glycine induce an inward current, with an amplitude of ~35 ± 21 pA. In contrast, the majority (86%, n = 50) of the glial cells with Na^+ currents, the presumptive astrocytic precursors, responded with currents of 58 ± 49 pA (Fig. 2). In the glial cells with Na^+ currents, the mean current amplitude was larger at P3–P8 than at P9–P14, i.e. 68 ± 57 (n = 31) and 38 ± 18 pA (n = 12) respectively (Fig. 2). GABA-activated inward currents were of similar amplitude in both types of glial cells, namely 517 ± 375 pA for the oligodendrocyte precursors (n = 28) and 465 ± 322 pA in glial cells with Na^+ currents (n = 35, Fig. 3).

Large GABA responses showed a complex time course. In the presence of GABA, rapid activation was followed by inactivation to an intermediate plateau, which returned to resting values after washout of GABA. Smaller responses observed in oligodendrocytes and astrocytes usually activated more slowly and terminated with the

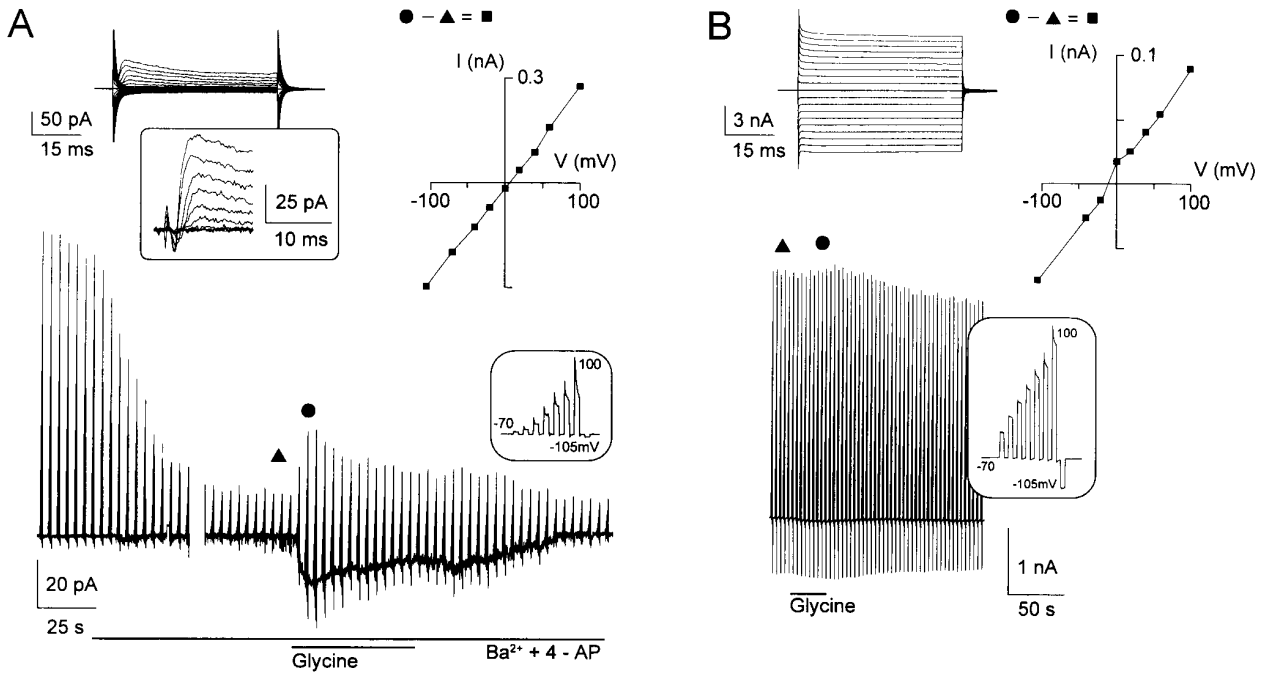

FIG. 4. Reversal potential of glycine induced currents. (A) The recordings were obtained from a glial cell with Na^+ currents [P3, resting membrane potential (V_r) −35 mV] The current pattern is shown on the upper left; currents were activated as described in the legend to Figure 1. The small inward Na^+ current was revealed after subtraction of leakage currents (see inset). Below, a series of depolarizing (–40, −20, 0, 20, 40, 60, 100 mV) and hyperpolarizing voltage steps (–105 mV) from a holding potential of −70 mV was applied repeatedly. The current response to one series of voltage steps is illustrated in the inset. Glycine was applied in the presence of the K^+ channel blockers Ba^{2+} (5 mM) and 4-AP (1 mM). The application of the K^+ channel blockers markedly reduced the outward currents. In their presence glycine induced a significant conductance increase and an inward current at −70 mV. To elucidate the glycine-induced conductance, currents prior to the application of glycine (triangle) were subtracted from currents at the peak of the glycine response (circle). The current–voltage curve of the glycine-induced current is linear and the reversal potential was close to 0 mV (upper right). (B) Similar recordings were obtained from an astrocyte (P7, V_r −77 mV). Each series of the voltage-clamp pattern appears as a single line in the current recording. Application of glycine induced an inward current at −70 mV and a conductance increase at de- and hyperpolarizing potential. Upper right is shown a plot of the glycine-induced current (I) as a function of holding potentials (V). The resulting current–voltage curve is almost linear and the reversal potential was −12 mV (upper right).

washout of the transmitter. Glial cells responding to glycine and GABA were found in all areas of the grey matter, including the dorsal and ventral horns, with no particular preference.

Glycine activates a Cl^- conductance

To identify the ionic species mediating the glycine-induced current response, cells with large responses were selected. For this purpose, the glial cells with Na^+ currents were particularly suitable since responses often exceeded 50 pA, and the resting K^+ conductance could be blocked by a combination of Ba^{2+} (5 mM) and 4-AP (1 mM). To study glycine-activated currents at different membrane potentials, the membrane was clamped at a series of potentials ranging between 100 and −105 mV. Each voltage step lasted for 100 ms and the series of voltage steps was applied every 3.6 s (Fig. 4A). Glycine-activated membrane currents were obtained by subtracting currents under control conditions from those at the peak of the glycine response. The resulting current–voltage curve was linear and reversed at 10.4 ± 10.6 mV (range 0–25 mV; n = 5), i.e. close to the Cl^- equilibrium potential (2 mV). The activation of ionic channels was further substantiated by the finding that current noise increased in the presence of glycine while the cell was clamped at −70 mV, as observed in the glial cells with Na^+ currents (n = 7).

In astrocytes and oligodendrocytes the analysis of the reversal potential was hampered by the large resting K^+ conductance, which could not be effectively blocked by the standard K^+ channel blockers. As a result, the reversal potential was usually more positive than 80 mV, indicating that the voltage-clamp control was insufficient. In three astrocytes, however, a reversal potential of −14 ± 2.8 mV was found (Fig. 4B). Seven glial precursor cells of the oligodendrocyte lineage showed glycine responses, and in one cell we determined a reversal potential of ~20 mV.

Glial glycine receptors are pharmacologically heterogeneous

The classical glycine receptor antagonist strychnine (10 μM) blocked or severely reduced the glycine-induced response to 6.3 ± 10% (n = 13; range 0–31%) compared to controls (Fig. 5). The blockade of the glycine responses was partially reversible to 49.6 ± 23.3% of the first glycine application (range 17–97%).

To pharmacologically characterize the glial glycine receptors further, we used picrotoxin (100 μM), which blocks (recombinant) glycine receptors containing no β subunit. In the glial cells with Na^+ currents, picrotoxin (100 μM) reversibly reduced the glycine (1 mM) response to 39.6 ± 9% (±SD, n = 4) (Fig. 6C). The response recovered to 87.3 ± 9.8% of the value prior to picrotoxin application. In four of seven astrocytes picrotoxin did not affect the glycine response (mean control value, 75 ± 30 pA), whereas in three astrocytes the glycine response (58 ± 53 pA) was reduced to 26 ± 28% with subsequent recovery to 68 ± 23% (Fig. 6B). In two of three oligodendrocytes picrotoxin did not influence the glycine response (mean 30 pA) (Fig. 6A), whereas in one oligodendrocyte

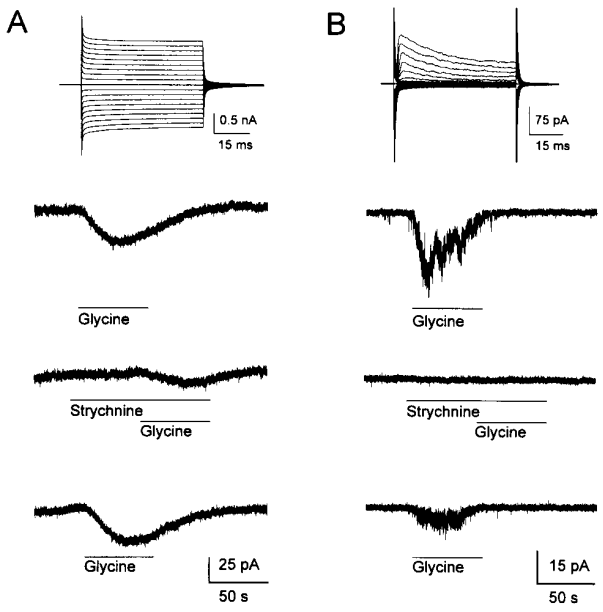

FIG. 5. Strychnine blocks the glycine response in rat spinal cord glial cells. (A) An oligodendrocyte [P8, resting membrane potential (V_r) −64 mV; membrane currents are shown in the inset as described in the legend to Fig. 1] was clamped at −70 mV while glycine (1 mM, bar) was applied. The control glycine responses before and after application of strychnine are displayed above and below. The glycine response was blocked in the presence of strychnine (10 μM, middle trace). Recordings were separated by 15 min. (B) A similar recording was obtained from a glial cell with Na^+ currents (P3, V_r −35 mV). As in the oligodendrocyte, strychnine reversibly blocked the glycine response.

the response (peak 63 pA) was slightly reduced to 76% followed by complete recovery. In nine of 11 neurons picrotoxin reduced the glycine response (195 ± 98 pA) to 38.4 ± 13.5%, which recovered to 80.3 ± 17.7%, whereas in the remaining two neurons the glycine response of 650 and 3000 pA was not affected in the presence of picrotoxin.

GABA activates a Cl^- conductance

The reversal potential of the GABA-activated current was determined by a current–voltage curve similar to that described for glycine. Prior to GABA application, the resting K^+ currents were blocked by the cocktail of Ba^{2+} (1 mM) and/or 4-AP (1 mM). The GABA-activated current was linear and reversed at −0.2 ± 15.3 mV, as determined for two astrocytes, two oligodendrocytes, one oligodendrocyte precursor, and five glial cells with Na^+currents. At the plateau phase, after the fast transient (see above), the current noise increased at the holding potential of −70 mV (n = 93). As shown in Figure 7A the voltage-activated currents became more apparent in the presence of Ba^{2+}/4-AP. One of two of these characterized cells was positively stained for GFAP, indicating that astrocytes in the spinal cord can express voltage-gated channels.

GABA blocks the resting K^+ conductance

With the resting K^+ conductance present (i.e. in the absence of K^+ channel blockers) GABA induced a complex response in the different glial populations. In the glial cells with Na^+ currents, a rapid conductance increase followed by a decrease in the outward conductance was observed in 51% of the cells (n = 29), as shown by the current–voltage curve of the GABA-activated current at the peak of the current increase (Fig. 8A, left): The conductance increased at potentials negative to −20 mV whereas at potentials more positive than −20 mV the conductance decreased. The decrease of the outward conductance lasted up to 3 min and could thus be isolated from the rapid transient conductance increase. The current–voltage curve of the conductance blocked by GABA yielded an activation threshold at potentials positive to −40 mV similar to the threshold of the (resting) delayed K^+ current (Fig. 8A, middle row). Subtracting the currents at the fast peak from those at the late phase yielded a reversal potential at ~0 mV; thus the Cl^- conductance could be isolated (Fig. 8A, right). We conclude that GABA induces two ionic mechanisms, the activation of a Cl^- conductance and a blockade of the resting K^+ conductance similar to that previously described for Bergmann glial cells (Müller *et al.*, 1994). The relative percentages of the two processes to each other, activation of the Cl^- conductance and the blockade of the K^+ conductance, varied among cells. If the Cl^- conductance activation was stronger than the K^+ conductance blockade, the reversal potential at the peak response was more positive than the Cl^- equilibrium potential (Fig. 8B). On the other hand, if more K^+ current was blocked than Cl^- current was activated, the reversal potential of the GABA-induced current was more negative than the K^+ equilibrium potential (Fig. 8A). In 33% of the glial cells with Na^+ currents (n = 15) the K^+ conductance block was stronger than the Cl^- conductance activation.

The transient increase and the sustained decrease in the membrane conductance was also observed in 20 of 38 astrocytes (Fig. 8B). In 14 of these 20 astrocytes, there was only a weak conductance increase, but a prominent decrease in the membrane conductance. In astrocytes, the current–voltage curve of the blocked current component was linear with a reversal potential close to the K^+ equilibrium potential, indicating the blockade of the resting (passive) K^+ conductance (Fig. 8B, middle).

A combined response—a conductance increase followed by a decrease—was also observed in five of 33 oligodendrocytes and in six of 21 oligodendrocyte precursor cells. The K^+ conductance block was stronger than the Cl^- conductance activation in 80% of the oligodendrocytes and in none of the oligodendrocyte precursors.

Cl^- conductance increase and blockade of the K^+ conductance are mediated by $GABA_A$ receptors

The GABA-evoked responses were blocked by bicuculline (100 μM), a $GABA_A$ receptor antagonist, in all glial cell types (Fig. 9A, B). Bicuculline blocked both the increase and the decrease in the membrane conductance (Fig. 9A, B). The bicuculline block was not fully reversible. This was most likely due to rundown of the GABA response which was often observed with repetitive applications even under control conditions, i.e. without antagonist. GABA responses were blocked to 18 ± 14% and recovered after washout of bicuculline to 45 ± 21% in astrocytes (n = 5), blocked to 17 ± 23% and recovered to 84 ± 39% in oligodendrocytes (n = 5), and blocked to 6 ± 5% and recovered to 46 ± 24% in oligodendrocyte precursor cells (n = 4); in glial cells with Na^+currents responses were blocked to 9 ± 4% and recovered to 37 ± 18% in glial cells (n = 3). The $GABA_A$ receptor agonist muscimol (100 μM) mimicked GABA responses in all cell types studied (astrocytes, n = 2; oligodendrocytes, n = 4; oligodendrocyte precursor cells, n = 3; glial cells with Na^+currents, n = 3) (Fig. 9C). Like GABA, muscimol induced a conductance increase with a reversal potential close to 0 mV and a

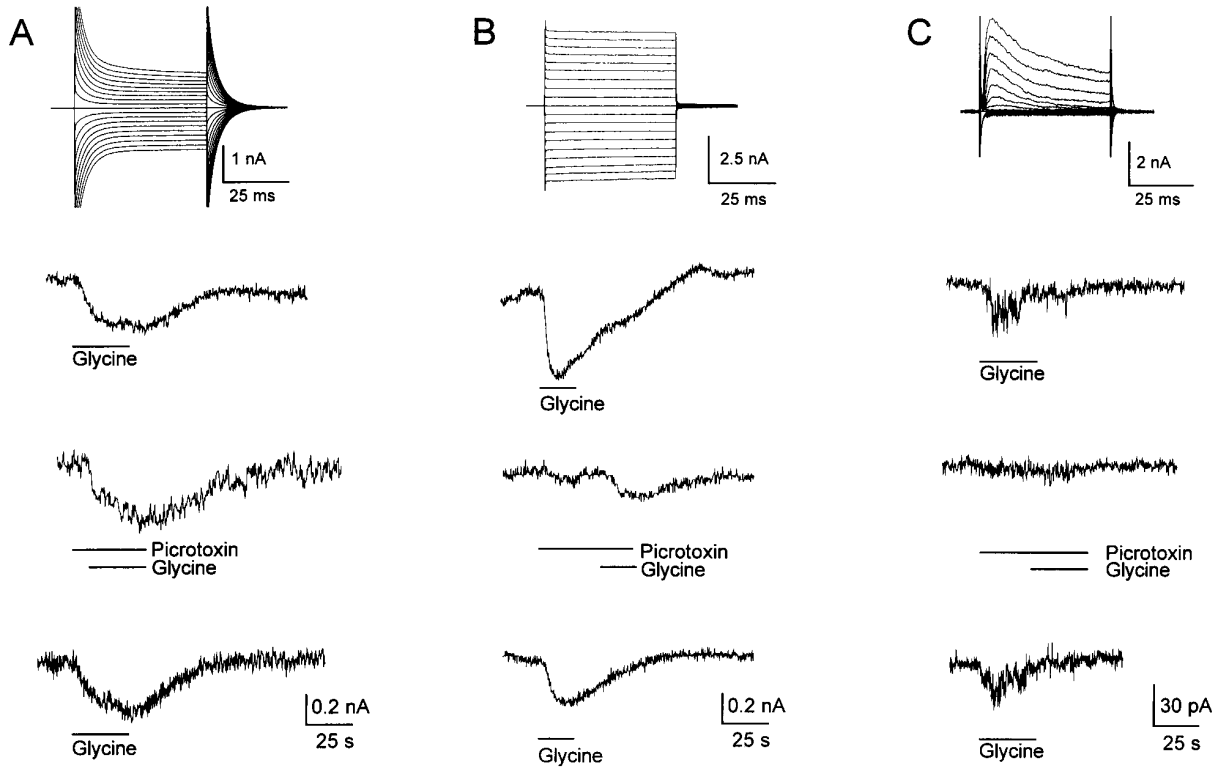

FIG. 6. Effect of picrotoxin on glycine-induced currents in rat spinal cord glial cells. (A) An oligodendrocyte [P9, resting membrane potential (V_r) −68 mV; voltage-gated currents as described in legend of Fig. 1, top] was clamped at −70 mV, while glycine (1 mM) was applied in the presence of the blocker picrotoxin (100 μM) (middle trace; bar indicates application). No effect of picrotoxin on the glycine response could be seen by comparison with control applications (upper trace, 10 min before picrotoxin washin; lower trace, 10 min after picrotoxin washout). (B) The same experiment as described in A was done with an astrocyte (P6, V_r −70 mV). Picrotoxin (500 μM) (middle trace) blocked the glycine response to 21% (control 120 pA, upper trace). After washout the glycine response recovered to 53% (lower trace). (C) A glial cell with Na^+ currents (P7, Vr −55 mV; membrane current pattern shown at the top is leak-subtracted). Picrotoxin (100 μM; middle trace) blocked the glycine response (control 30 pA, upper trace). After washout the glycine response recovered to 81% (lower trace).

decrease in K^+ currents activated with membrane depolarization (Fig. 9C). Usually, the inward current (at a membrane potential of −70 mV) activated by muscimol was larger than the GABA-activated current. We conclude that both the activation of the Cl^- conductance and the blockade of the K^+ conductance are mediated by $GABA_A$ receptors.

To further characterize the GABA receptors in the spinal cord astrocytes, we used the β-carboline DMCM, which modulates GABA responses differently in cultured astrocytes and oligodendrocytes (Blankenfeld and Kettenmann, 1992). The membrane was clamped at −70 mV, and the GABA-activated currents in the presence of DMCM (10 μM, with 60 s preincubation) were compared to control responses before and after (Fig. 10). The GABA response in the presence of DMCM was reversibly reduced in all cell types. The responses were reduced to 43 ± 32% and recovered to 80 ± 12% in astrocytes (n = 5) (Fig. 10A), reduced to 50% and recovered to 83% in oligodendrocytes (n = 1), and reduced to 35 and 66% in two glial cells with Na^+currents and recovered to 65 and 70%. A similar effect was observed in two spinal cord neurons, where the GABA responses were reduced to 40 and 65% and recovered to 60 and 70% (Fig. 10B).

Discussion

GABA and glycine receptors in glial cells

In this study we demonstrate that the neurotransmitters glycine and GABA mediate currents in glial cells of the rat spinal cord slice. So far the presence of glycine receptors on glial cells has not been described; in contrast glial GABA receptors have been described in a variety of glial cell types. Glial $GABA_A$ receptors were first discovered in cultured astrocytes and oligodendrocytes (Gilbert *et al.*, 1984; Kettenmann *et al.*, 1984) and subsequently in *in situ* preparations, e.g. in astrocytes from slices of the rat hippocampus (MacVicar *et al.*, 1989; Steinhäuser *et al.*, 1994), in oligodendrocytes from the corpus callosum (Berger *et al.*, 1992), and in Bergmann glial cells of the cerebellum (Müller *et al.*, 1994). The presence of GABA receptors in the spinal cord glial cells is substantiated by the pharmacological profile of the GABA-induced current and by its biophysical properties in that it induced a membrane conductance increase with a reversal potential at the Cl^- equilibrium. Moreover, a noise increase was observed during GABA application, indicating the activation of ionic channels. Taken together, these results demonstrate that rat spinal cord glial cells express $GABA_A$ type receptors.

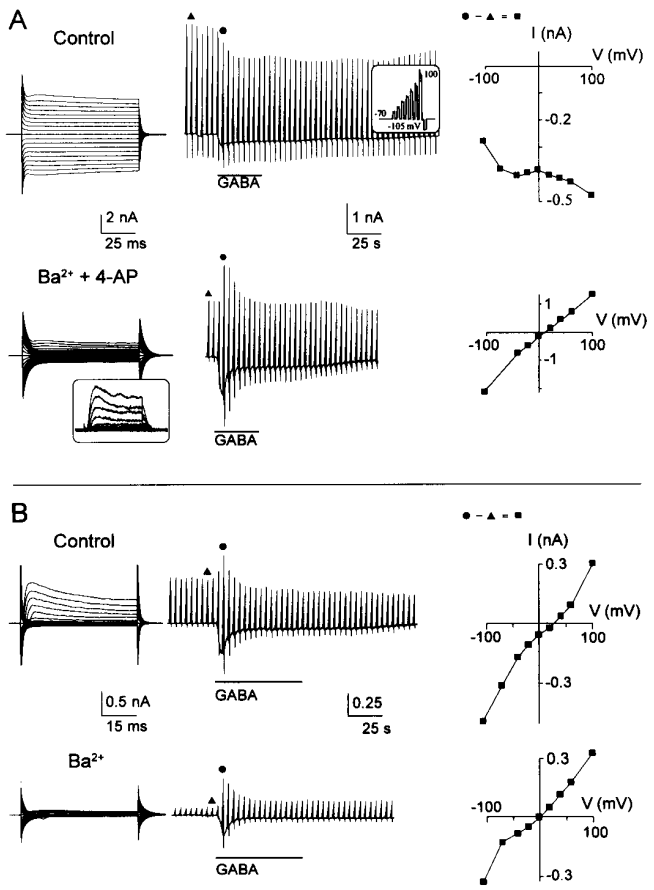

FIG. 7. Reversal potentials of GABA induced membrane currents. (A) An astrocyte [P6, resting membrane potential (V_r) −79 mV] was characterized by its morphology and current pattern; currents were activated as described in the legend to Figure 1 (left trace). Middle lane: the membrane potential was clamped to a series of de- and hyperpolarizing values in a repetitive manner as described in Figure 4. GABA (1 mM, bar indicates application) induced a decrease in membrane conductance. The GABA-sensitive current was obtained by subtracting control currents (triangle) from those at the peak of the response (circle). The resulting current–voltage curve is shown on the right. A similar set of recordings was obtained from the same cell in the presence of the K^+ channel blockers Ba^{2+} (5 mM) and 4-AP (1 mM). In Ba^{2+} and 4-AP the cell depolarized from −79 to −62 mV, indicating that currents that were non-selective for K^+ had become more prevalent. GABA induced a conductance increase which reversed at ~6 mV. The currents in the inset are leakage-corrected outward currents. (B) A glial cell with Na^+ currents (P5, V_r −38 mV; left trace; currents were activated as described in the legend to Fig. 1) was characterized as described in A. In control solution the reversal potential of the GABA-induced current is ~30 mV, whereas in 5 mM Ba^{2+} it is shifted to 0 mV.

The GABA response seems to be down-regulated in more mature glial cells. The presumed astrocyte precursor cells, the glial cells with Na^+ currents, and the oligodendrocyte precursor cells have large GABA-induced currents, indicating a higher density of $GABA_A$ receptors in the cell membrane. In contrast, the current response in oligodendrocytes and in astrocytes older than P9 was about one order of magnitude smaller. This implies that GABA receptors are either substantially less dense or that the receptors are located at remote membrane areas, e.g. at the tip of processes, which are not controlled by our voltage-clamp system. Indeed, such an uneven distribution—the presence of the receptors on the processes—has been described

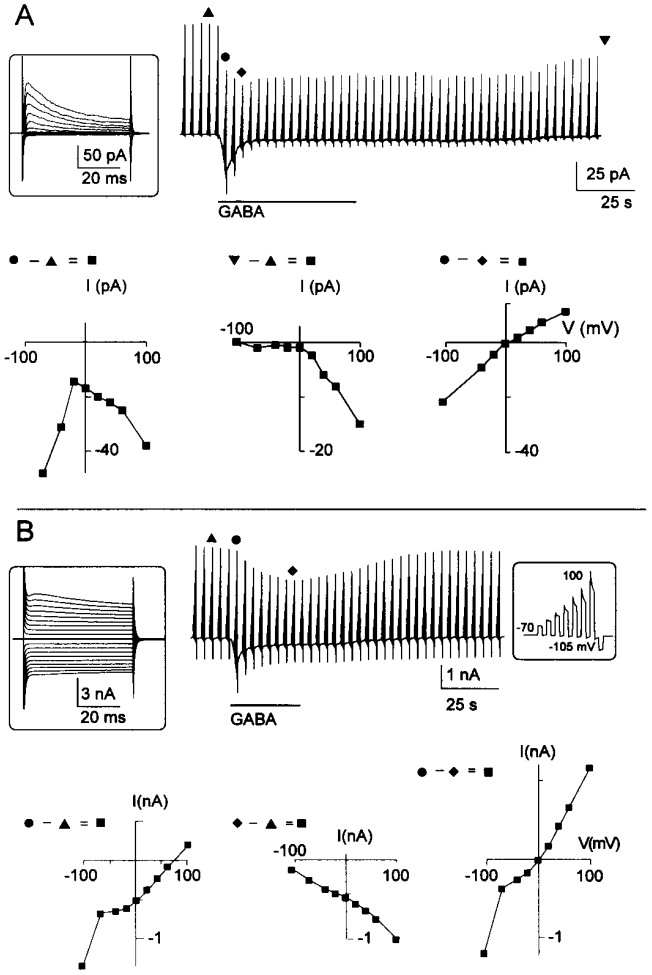

FIG. 8. GABA blocks the resting K+ conductance. (A) In a glial cell with Na^+ currents [P5, resting membrane potential (V_r) −43 mV] GABA induced a conductance increase followed by a substantial conductance decrease. The inset (top left) illustrates the membrane currents described in Figure 1. The GABA response was recorded with a protocol of voltage steps as described in Figure 4. To analyse the ionic mechanism underlying these changes, three types of current–voltage curves were constructed. (i) Control currents were subtracted from the GABA-induced currents at the peak of the inward current (triangle − circle). The resulting current–voltage curve shows a current increase at hyperpolarizing potentials and a conductance decrease at potentials positive to −20 mV (bottom left). (ii) Control currents were subtracted from the currents at the maximal conductance decrease ~2.5 min after the onset of the GABA response (base-up triangle − base-down triangle; bottom middle). The resulting current–voltage curve shows the blockade of the K_{DR} current. (iii) The subtraction of currents at the maximal conductance decrease from currents at maximal conductance increase (circle − rhombus; bottom right) resulted in a current–voltage curve with a reversal potential of 0 mV. (B) An experiment similar to that described in A was carried out on an astrocyte (P7, V_r −63 mV). The cell was positively identified by GFAP staining (not shown). The membrane current pattern was obtained as described in Figure 1 and is illustrated in the inset on the left. One sequence of voltage steps for the recording during GABA application (middle) is shown on the right. GABA induced a substantial decrease in membrane conductance. (i) The subtraction of control currents from currents at the peak GABA response (circle − triangle, bottom left) led to a current–voltage curve with a reversal potential of ~75 mV. (ii) The membrane conductance decrease was isolated by the subtraction of control currents from the currents at maximal conductance decrease ~30 s after the onset of the GABA response (rhombus − triangle, bottom middle). (iii) Subtracting currents at the peak conductance decrease from the currents at the peak conductance increase (circle − rhombus, right) led to a current–voltage curve with a reversal potential of 0 mV.

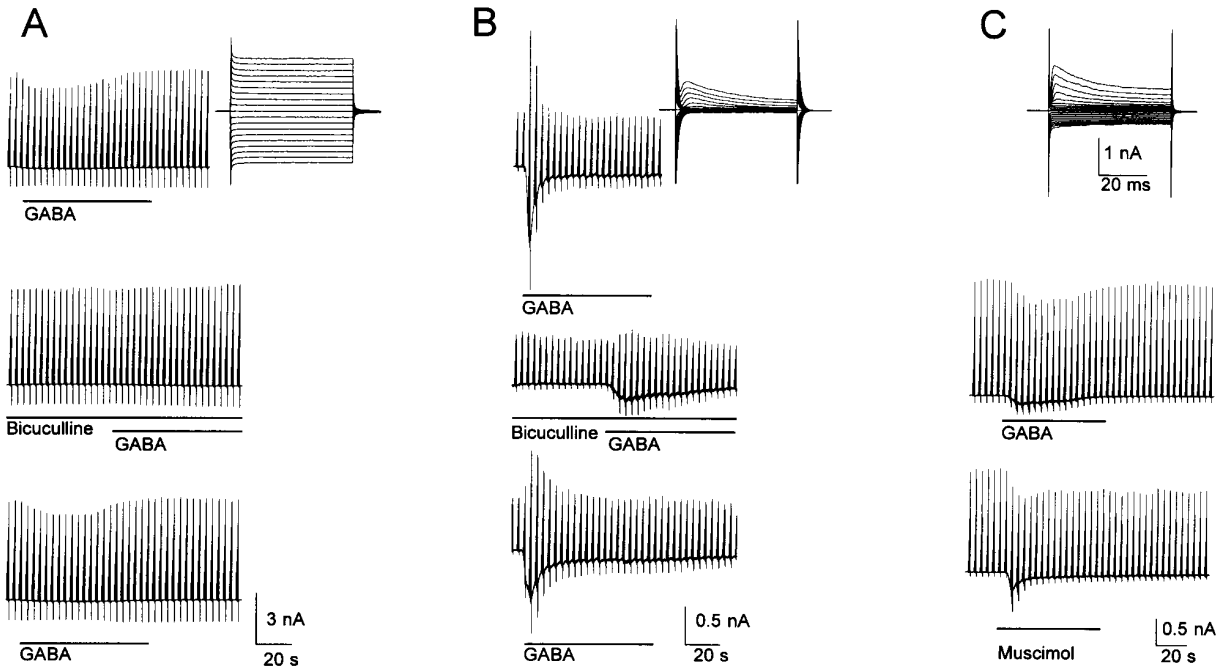

FIG. 9. Effect of muscimol and modulation of GABA responses by bicuculline. (A) GABA responses were obtained from an astrocyte with the voltage-clamp pattern as described in Figure 3 [P13, resting membrane potential (V_r) −72 mV; voltage-activated current pattern as described in Figure 1, upper right]. A control application of GABA (1 mM, upper trace), in the presence of bicuculline (100 μM, middle trace) and after washout of bicuculline. Bicuculline blocked the conductance decrease in a reversible manner. (B) In a glial cell with Na^+ currents (P14, V_r −43 mV), GABA (1 mM) induced a conductance increase under control conditions (upper trace). This conductance increase was blocked in the presence of bicuculline (100 μM) and partially recovered after the washout (lower trace). (C) In a glial cell with Na^+ currents (P5, V_r −65 mV), GABA (100 μM) induced a conductance decrease (middle trace) which could be mimicked by muscimol (100 μM, lower trace).

for Bergmann glial cells (Müller *et al.*, 1994). On the other hand, a decreasing density of $GABA_A$ receptors during development has been described for cultured optic nerve astrocytes (Ochi *et al.*, 1993).

Pharmacological properties of GABA receptors in the spinal cord

GABA-induced currents in glial cells of the rat spinal cord slice share many pharmacological properties with neuronal $GABA_A$ receptors. The response can be mimicked by the $GABA_A$ receptor agonist muscimol, and it can be blocked by the antagonist bicuculline. Heterogeneity is introduced with respect to its benzodiazepine pharmacology. GABA receptors in cultured astrocytes are distinct from those in neurons and oligodendrocytes in that the inverse benzodiazepine agonist DMCM reduced the current in the latter and augmented it in the former (Backus *et al.*, 1988; Bormann and Kettenmann, 1988). This distinct behaviour was also found in astrocytes from acutely isolated hippocampal astrocytes, though in only 20% of the cells (Fraser *et al.*, 1995), and in a subpopulation of cultured rat spinal cord astrocytes; the latter study revealed that in protoplasmic astrocytes DMCM augmented GABA-activated currents, while in fibrous astrocytes a decrease was observed (Rosewater and Sontheimer, 1994).

The inverse benzodiazepine agonist DMCM reduced the GABA response in all rat spinal cord glial cells and neurons tested, suggesting that the $GABA_A$ receptors of these cells contain the neuronal γ2 subunit. This implies that we have either recorded from cells of the oligodendrocyte lineage or from the fibrous astrocyte lineage. We were either not yet able to patch protoplasmic astrocytes in the spinal

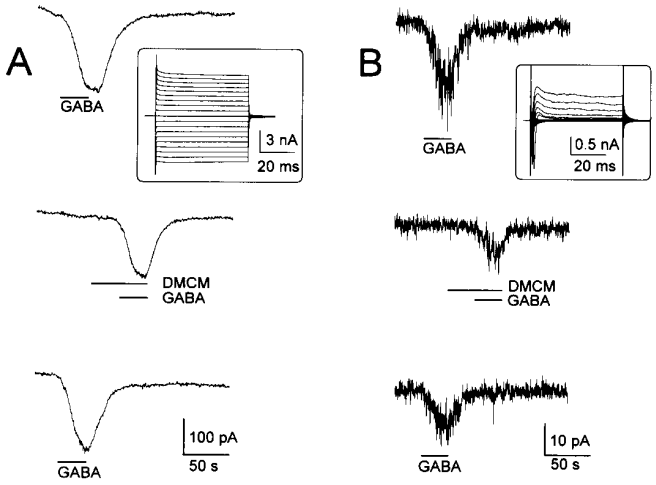

FIG. 10. Effect of DMCM on GABA-activated currents. (A) An astrocyte [P7, resting membrane potential (V_r) −77 mV; voltage-gated currents as described in the legend to Fig. 1 are shown in the inset] was clamped at −70 mV while GABA (10 μM) was applied in the presence of DMCM (10 μM; bar indicates application) (middle trace). The comparison with control GABA responses (upper trace, 10 min before DMCM; bottom trace, 10 min after washout of DMCM) shows that DMCM reduced the GABA responses. (B) The same experiment as described in A was done with a neuron (P5, V_r −57 mV). In the presence of DMCM the GABA response was reduced.

cord slice, or the DMCM-induced increase of the GABA response is only a property of cultured protoplasmic astrocytes.

Properties of glial glycine receptors

The glycine induced currents in rat spinal cord glial cells share many features with responses mediated by glycine receptors. The reversal potential of the response was close to the Cl^- equilibrium potential, an increase in current noise was observed in some experiments and the specific antagonist strychnine blocked the response. We therefore conclude that astrocytes and oligodendrocytes, as well as glial precursor cells from the spinal cord slice, can express glycine receptors at P3–P18.

The GABA receptor Cl^- channel blocker picrotoxin can be used to distinguish between different types of glycine receptors. Picrotoxin was found to block glycine responses in recombinant homomeric α glycine receptors (Schmieden *et al.*, 1989; Sontheimer *et al.*, 1989; Pribilla *et al.*, 1992). The picrotoxin resistance of the glycine-induced currents has been correlated with the M2 segment of the β subunit of the glycine receptor (Pribilla *et al.*, 1992). *In vivo*, the situation is heterogeneous. Picrotoxin blockade of glycine-induced currents has been observed in neurons of the developing brain and in primary culture (Hill *et al.*, 1976; Mori-Okamoto and Tatsuno, 1985; Soffe, 1987; Akaike and Kaneda, 1989). In neurons of the adult spinal cord no inhibition is seen (Pribilla *et al.*, 1992). Though Evans (1978) measured no picrotoxin sensitivity in motoneurons and primary afferent terminals in isolated spinal cord of young rats, biochemical data on cultured neurons from rodent spinal cord suggest that the neonatal glycine receptor isoform prevalent at birth may be a homo-oligomer of α2 subunits (Hoch *et al.*, 1989).

In the rat spinal cord from P6 to P9 we observed picrotoxin blockade of the glycine response in 92% of the neurons, suggesting an embryonic homomeric α isoform of the glycine receptor which later during development is replaced by the heteromeric aβ form.

In all spinal cord glial cells with Na^+ currents picrotoxin reversibly blocked the glycine-induced currents whereas in astrocytes and oligodendrocytes heterogeneity was found. In three astrocytes and in one oligodendrocyte picrotoxin blocked the glycine response whereas it did not affect the glycine-induced current in other astrocytes and oligodendrocytes, all obtained from the same developmental stage (P6–P9).

This implies that the glycine receptors in glial cells undergo changes during development; glial precursor cells are picrotoxin-sensitive and thus most likely lack the β subunit. In contrast, astrocytes and oligodendrocytes become at least partially picrotoxin-insensitive, indicating the incorporation of the β subunit into the receptor complex.

GABA receptor activation and K^+ channel blockade

In addition to triggering a Cl^- channel, the activation of the $GABA_A$ receptor of spinal cord glial cells leads to blockade of the (resting) K^+ conductance. This effect is mediated by $GABA_A$ receptors since the K^+ channel blockade was not observed in the presence of the $GABA_A$ receptor antagonist bicuculline and was mimicked by the specific agonist muscimol. A similar mechanism has been described for Bergmann glial cells (Müller *et al.*, 1994). The link between receptor activation and modulation of K^+ channel activity is unknown. So far, such an effect of GABA has only been observed in glial cells. Activation of second messenger systems by $GABA_A$ receptors has not been described; an exception is the Ca^{2+} influx mediated by the GABA-induced membrane depolarization and the subsequent activation of Ca^{2+} channels as described for immature neurons and glial precursor cells (Connor *et al.*, 1987; Kirchhoff and Kettenmann, 1992). The involvement of Ca^{2+} mobilization via voltage-gated channels in the K^+ channel blockade is unlikely, since the cells were clamped at the resting membrane potential and a depolarization could only occur at membrane areas which were not under voltage-clamp control. An alternative mechanism could be mediated by the flux of Cl^- or HCO_3^-, resulting in changes in internal pH, Cl^- or other ions.

Glial receptors and synaptic transmission

Glial cells closely interact with synapses by insulating the pre-and postsynaptic complex (Baude *et al.*, 1994). This interaction points to a functional involvement in synaptic transmission. Indeed, the impairment of glial function blocks synaptic transmission in the guinea-pig hippocampal slice (Keyser and Pellmar, 1994). Modulation of synaptic function could be mediated by morphological changes of the glial cells at the synaptic regions. Glial receptors activated by transmitter escaping from the synaptic cleft could result in a structural change of the glial synaptic ensheathment. Such morphological changes upon neurotransmitter activation have been described for cultured astrocytes and were observed in glial processes after long-term potentiation (Cornell-Bell *et al.*, 1990; Wenzel *et al.*, 1991). The finding that rat spinal cord glial cells express glycine receptors further supports the concept that glial cells are equipped with the sensors to detect synaptic activity of their environment. Glial glycine responses have so far not been detected in glial cells from other brain areas or in culture. Since glycine receptors are most abundant in the spinal cord compared to other brain regions, the concept emerges that glial cells need to express the appropriate receptor repertoire to participate in synaptic communication.

Acknowledgements

This work was supported by the Deutsche Forschungsgemeinschaft (SFB 317), by the Bundesministerium für Forschung und Technologie, by the Graduiertenfoerderung Baden-Wuerttemberg, and by the Grant Agency of the Czech Republic (grant 309/93/1048).

Abbreviations

4-AP	4-aminopyridine
DMCM	methyl-6,7-dimethoxy-4-ethyl-β-carboline-3-carboxylate
EGTA	ethyleneglycol-bis-(β-aminoethyl ether)-*N,N,N′,N′*-tetraacetic acid
GABA	γ-aminobutyric acid
GFAP	glial fibrillary acidic protein
HEPES	*N*-(2-hydroxyethyl)piperazine-*N′*-(2-ethanesulphonic acid)
K_A	A-type potassium current
K_{DR}	delayed rectifying potassium current
K_{IR}	inward rectifying potassium current
O1, O4	antibodies for glial cells of the oligodendrocyte lineage
P	postnatal day

References

Akaike, N. and Kaneda, M. (1989) Glycine-gated chloride current in acutely isolated rat hypothalamic neurons. *J. Neurophysiol.*, **62**, 1400–1409.

Backus, K. H., Kettenmann, H. and Schachner, M. (1988) Effect of benzodiazepines and pentobarbital on the GABA-induced depolarization in cultured astrocytes. *Glia*, **1**, 132–140.

Baude, A., Molnar, E., Latawiec, D., McIlhinney, R. A. J. and Somogyi, P. (1994) Synaptic and nonsynaptic localization of the GluR1 subunit of the AMPA-type excitatory amino acid receptor in the rat cerebellum. *J. Neurosci.*, **14**, 2830–2843.

Berger, T., Schnitzer, J. and Kettenmann, H. (1991) Developmental changes in the membrane current pattern, K^+ buffer capacity, and morphology of glial cells in the corpus callosum slice. *J. Neurosci.*, **11**, 3008–3024.

Berger, T., Walz, W., Schnitzer, J. and Kettenmann, H. (1992) GABA and

glutamate activate currents in glial cells of the corpus callosum slice. *J. Neurosci. Res.*, **31**, 21–27.

Blankenfeld, G. and Kettenmann, H. (1992) Glutamate and GABA receptors in vertebrate glial cells. *Mol. Neurobiol.*, **5**, 31–41.

Bormann, J. and Kettenmann, H. (1988) Patch clamp study of gamma-aminobutyric acid receptor Cl^- channels in cultured astrocytes. *Proc. Natl Acad. Sci. USA*, **85**, 9336–9340.

Chvátal, A., Pastor, A., Mauch, M., Syková, E. and Kettenmann, H. (1995) Distinct populations of identified glial cells in the developing rat spinal cord slice: ion channel properties and cell morphology. *Eur. J. Neurosci.*, **7**, 129–142.

Condorelli, D. F., Ingrao, F., Magri, G., Bruno, V., Nicoletti, F. and Avola, R. (1989) Activation of excitatory amino acid receptors reduces thymidine incorporation and cell proliferation rate in primary cultures of astrocytes. *Glia*, **2**, 67–69.

Connor, J. A., Tsengo, H. Y. and Hockberger, P. E. (1987) Depolarization and transmitter induced changes in intracellular Ca^{2+} of rat cerebellar granule cells in explant cultures. *J. Neurosci.*, **7**, 1384–1400.

Cornell-Bell, A. H., Thomas, P. G. and Smith, J. (1990) The excitatory neurotransmitter glutamate causes filopodia formation in cultured hippocampal astrocytes. *Glia*, **3**, 332–334.

Debus, E., Weber, K. and Osborn, M. (1983) Monoclonal antibodies specific for glial fibrillary acidic (GFA) protein and for each of the neurofilament triplet polypeptides. *Differentiation*, **25**, 193–203.

Dodt, H. U., Pawelzik, H. and Zieglgaensberger, W. (1989) Infrared DIC videomicroscopy of living brain slices. *Soc. Neurosci. Abstr.*, **15**, 280.

Edwards, F. A., Konnerth, A., Sakmann, B. and Takashaki, T. (1989) A thin slice preparation for patch-clamp recordings from neurons of the mammalian central nervous system. *Pflügers Arch.*, **414**, 600–612.

Eng, L. F., Vanderhaegen, J. J., Bignami, A. and Gerstl, B. (1971) An acidic protein isolated from fibrous astrocytes. *Brain Res.*, **28**, 351–354.

Evans, R. H. (1978) The effects of amino acids and antagonists on the isolated hemisected spinal cord of the immature rat. *Br. J. Pharmacol.*, **62**, 171–176.

Fraser, D. D., Duffy, S., Angelides, K. J., Velazquez, J.-L. P., Kettenmann, H. and MacVicar, B. A. (1995) $GABA_A$/benzodiazepine receptors in acutely isolated hippocampal astrocytes. *J. Neurosci.*, in press.

Giaume, C., Marin, P., Cordier, J., Glowinski, J. and Premont, J. (1991) Adrenergic regulation of intercellular communications between cultured striatal astrocytes from the mouse. *Proc. Natl Acad. Sci. USA*, **88**, 5577–5581.

Gilbert, P., Kettenmann, H. and Schachner, M. (1984) γ-Aminobutyric acid directly depolarizes cultured oligodendrocytes. *J. Neurosci.*, **4**, 561–569.

Hamill, O. P., Marty, E., Neher, E., Sakmann, B. and Sigworth, F. J. (1981) Improved patch clamp techniques for high resolution current recording from cells and cell-free membrane patches. *Pflügers Arch.*, **391**, 85–100.

Hill, R. G., Simmonds, M. A. and Straughan, D. W. (1976) Antagonism of γ-aminobutyric acid and glycine by convulsants in the cuneate nucleus of cat. *Br. J. Pharmacol.*, **56**, 9–19.

Hoch, W., Betz, H. and Becker, C.-M. (1989) Primary cultures of mouse spinal cord express the neonatal isoform of the inhibitory glycine receptor. *Neuron*, **3**, 339–348.

Jendelova, P. and Syková, E. (1991) Role of glia in K^+ and pH homeostasis in the neonatal rat spinal cord. *Glia*, **4**, 56–63.

Keyser, D. O. and Pellmar, T. C. (1994) Synaptic transmission in the hippocampus: critical role for glial cells. *Glia*, **10**, 237–243.

Kettenmann, H., Sonnhof, U. and Schachner, M. (1983) Exclusive potassium dependence of the membrane potential in mouse oligodendrocytes. *J. Neurosci.*, **3**, 500–505.

Kettenmann, H., Sonnhof, U., Camerer, H., Kuhlmann, S., Orkand, R. K. and Schachner, M. (1984) Electrical properties of oligodendrocytes in culture. *Pflügers Arch.*, **40**, 324–332.

Kirchhoff, F. and Kettenmann, H. (1992) GABA triggers a $[Ca^{2+}]_i$ increase in murine precursor cells of the oligodendrocyte lineage. *Eur. J. Neurosci.*, **4**, 1049–1058.

MacVicar, B. A., Tse, F. W. Y., Crichton, S. A. and Kettenmann, H. (1989) GABA-activated Cl^- channels in astrocytes of hippocampal slices. *J. Neurosci.*, **9**, 3577–3583.

Mori-Okamoto, J. and Tatsuno, J. (1985) Development of sensitivity to GABA and glycine in cultured cerebellar neurons. *Brain Res.*, **352**, 249–258.

Müller, T., Fritschy, J. M., Grosche, J., Pratt, G. D., Möhler, H. and Kettenmann, H. (1994) Developmental regulation of voltage-gated K^+ channel and $GABA_A$ receptor expression in Bergmann glial cells. *J. Neurosci.*, **14**, 2503–2514.

Ochi, S., Lim, J. Y., Rand, M. N., During, M. J., Sakatani, K. and Kocsis, J. D. (1993) Transient presence of GABA in astrocytes of the developing optic nerve. *Glia*, **9**, 188–198.

Pribilla, I., Takagi, T., Langosch, D., Bormann, J. and Betz, H. (1992) The atypical M2 segment of the β subunit confers picrotoxinin resistance to inhibitory glycine receptor channels. *EMBO J.*, **11**, 4305–4311.

Rosewater, K. and Sontheimer, H. (1994) Fibrous and protoplasmic astrocytes express $GABA_A$ receptors that differ in benzodiazepine pharmacology. *Brain Res.*, **636**, 73–80.

Schmieden, V., Grenningloh, G., Schofield, P. R. and Betz, H. (1989) Functional expression in *Xenopus* oocytes of the strychnine binding 48 kD subunit of the inhibitory glycine receptor. *Biochemistry*, **30**, 42–47.

Sommer, I. and Schachner, M. (1981) Monoclonal antibodies (O1 to O4) to oligodendrocyte cell surfaces: an immunocytological study in the central nervous system. *Dev. Biol.*, **83**, 311–323.

Sontheimer, H. and Kettenmann, H. (1988) Heterogeneity of potassium currents in cultured oligodendrocytes. *Glia*, **1**, 415–420.

Sontheimer, H. and Waxman, S. G. (1992) Ion channels in spinal cord astrocytes *in vitro*. II. Biophysical and pharmacological analysis of Na^+ currents. *J. Neurophysiol.*, **68**, 1001–1011.

Sontheimer, H., Becker, C.-M., Pritchett, D., Schofield, P., Grenningloh, G., Kettenmann, H., Betz, H. and Seeburg, P. (1989) Functional chloride channels by mammalian cell expression of rat glycine receptor subunit. *Neuron*, **2**, 1491–1497.

Sontheimer, H., Black, J. A., Ransom, B. R. and Waxman, S. G. (1992) Ion channels in spinal cord astrocytes *in vitro*. I. Transient expression of high levels of Na^+ and K^+ channels. *J. Neurophysiol.*, **68**, 985–1000.

Soffe, S. R. (1987) Ionic and pharmacological properties of reciprocal inhibition in *Xenopus* embryo motoneurones. *J. Physiol. (Lond.)*, **382**, 463–473.

Steinhäuser, C., Jabs, R. and Kettenmann, H. (1994) Properties of GABA and glutamate responses in identified glial cells of the mouse hippocampal slice. *Hippocampus*, **4**, 19–36.

Syková, E. and Chvátal, A. (1993) Extracellular ionic and volume changes: the role in glia–neuron interaction. *J. Chem. Neuroanat.*, **6**, 247–260.

Syková, E., Jendelová, P., Simonová, Z. and Chvátal, A. (1992) K^+ and pH homeostasis in the developing rat spinal cord is impaired by early postnatal X-irradiation. *Brain Res.*, **594**, 19–30.

Thio, C. L., Waxman, S. G. and Sontheimer, H. (1993) Ion channels in spinal cord astrocytes *in vitro*. III. Modulation of channel expression by coculture with neurons and neuron-conditioned medium. *J. Neurophysiol.*, **69**, 819–831.

Wenzel, J., Lammert, U. and Krug, M. (1991) The influence of long-term potentiation on the spatial relationship between astrocyte processes and potentiated synapses in the dentate gyrus neuropil of rat brain. *Brain Res.*, **560**, 122–131.